GEOPHYSICAL RESEARCH LETTERS, VOL. 24, NO.13, PAGES 1603-1606, JULY 1, 1997

Solitary waves in the western Equatorial Pacific Ocean

R. Pinkel,[1] M. Merrifield,[2] M. McPhaden,[3] J. Picaut,[4] S. Rutledge,[5] D. Siegel,[6] and L. Washburn[6]

Abstract. During the spring tides of early January and February 1993, groups of solitary internal waves were observed propagating through the Intensive Flux Array of the TOGA COARE experiment. The waves appear to originate near the islands of Nugarba (3°S 30'S - 154° 30'E). They travel north-eastward at 2.5-3 m/s, closely coupled with the semi-diurnal baroclinic tide. Peak amplitudes exceed 60 m. Velocities are in excess of .8 m/s. Sea-surface vertical displacements of order .3 m can be inferred directly from the lateral acceleration of surface waters. The Equatorial Undercurrent is displaced by soliton passage but apparently is unaffected otherwise. The intrinsic shear of the solitary crests is small compared to ambient equatorial shears. The crests, while not themselves unstable, are effective at triggering instabilities on the background flow. The motions potentially contribute 10-15 Watts/m^2 to the flux of heat into the mixed layer.

1. Introduction

From November 1992 through February 1993 a multi-national air-sea interaction experiment was conducted in the Western Equatorial Pacific. Termed the Intensive Observation Period (IOP) of TOGA COARE (Webster and Lukas, 1992), the experiment involved ship, aircraft and land-based observations. The COARE intensive Flux Array (IFA) was centered at 2°S, 156°E over the 2 km deep Ontong Java Plateau (Fig. 1a,b). The surface waters of this region are among the warmest on the planet. Fluctuations in the state of the so-called "Warm Pool" and the overlying atmosphere are linked to subsequent climatic fluctuations eastward along the equator and at higher latitudes. Numerous oceanographic sensors were deployed in COARE to investigate processes which regulate the heat exchange between the warm surface waters and the cooler waters below.

A major surprise was the discovery of large (60 m) amplitude internal solitary waves propagating toward the northeast through the COARE IFA during periods of spring tide. Such waves are often seen on continental shelves, generated by tidal flow around coastal topography (Haury et al., 1979, Holloway, 1987, Sandstrom and Elliot, 1984. Fewer observations of deep sea solitary waves exist (Osborne and Burch, 1980, Apel et al., 1985, New and Pingree, 1990). Deep-ocean solitons propagate faster than their coastal counterparts and can be an order of magnitude more energetic. Their generation mechanism, interaction with the ambient environment, and ultimate fate are the subjects of present conjecture.

The COARE observations are of particular interest in that the solitons pass through an oceanographic region of extreme complexity. The South Equatorial Current (0-80 m depth, westward flow) and the Equatorial Undercurrent (160-250 m depth, eastward flow) dominate the large-scale background. The observations provide an ideal opportunity to investigate the interaction between the solitons and the ambient environment. Indeed, as distinct and significant perturbations, the solitons can provide insight into the stability of the pre-existing flows. Here we present data representative of the observed encounters.

2. Observations

The first observation of a well defined soliton was on 28 November, 1992. The Doppler sonar on the R/V Vickers (2°S, 156°15' E) detected passage of a single 40 m downward pointing "crest" at 1400 UTC. During the spring tides of 7-9 January and 8-11 February 1993, numerous solitary waves transited the COARE domain. A clear signature of event passage can be seen in ship's navigational records (Fig. 1c). For example, on 11 January 1993, the predominately southwestward drift of the R/V Vickers was interrupted by successive 1000 m displacements toward the northeast as the ship was advected by passing wave crests.

In conditions of moderate wind, the solitary waves strain the sea-surface sufficiently to modify the propagation of short gravity waves. The disturbance is often adequate to produce a pattern visible to the eye, to ship's radar, and to the advanced meteorological radars fielded in COARE (Fig. 1d). The propagation speed of the events, ~2.5 m s^{-1}, can be inferred from the time evolution of these radar images. Wavefronts can extend 50 km.

A consistent record of wave passage is obtained from the Vickers Doppler sonar, which operated throughout the COARE IOP. The sonar, designed and constructed at SIO, transmits repeat sequence coded pulses (Pinkel and Smith, 1992) every .6 sec. at 161 kHz. Profiles of ocean velocity and acoustic scattering strength are obtained with a resolution of 2.5 m in depth, 2 min. in time to depths in excess of 200 m. An inertial reference sensor is interfaced to the sonar processor, such that data are averaged in constant depth bins, independent of the instantaneous roll of the ship. To convert to absolute velocity, sonar data are combined with ship velocity estimates obtained from a Magnavox 4200 C/A code GPS receiver.

Six packets of solitons traversed the COARE domain between 23:00 UTC on 9 January and 22:00 UTC on 11 January. The subsequent baroclinic tidal waveform was significantly non-sinusoidal, although neither solitary wave nor bore-like behavior was observed. The January packets consisted of 2,2,2,3,3 and 2 distinct crests, respectively, occurring at 12.4 hr intervals. In

[1] Robert Pinkel, Scripps Inst. of Oceanography, code 0213, La Jolla, CA 92093-0213
[2] M. Merrifield
University of Hawaii, Honolulu, Hawaii
[3] M. McPhaden
Pacific Marine Environmental Laboratory, NOAA, Seattle, WA
[4] J. Picaut
Groupe SURTROPAC, ORSTOM, Noumea, New Caledonia
[5] S. Rutledge
Colorado State University, Fort Collins, Colorado
[6] D. Siegel and L. Washburn
University of California Santa Barbara, Santa Barbara, CA

Paper number 97GL01610.
0094-8534/97/97GL-01610$05.00

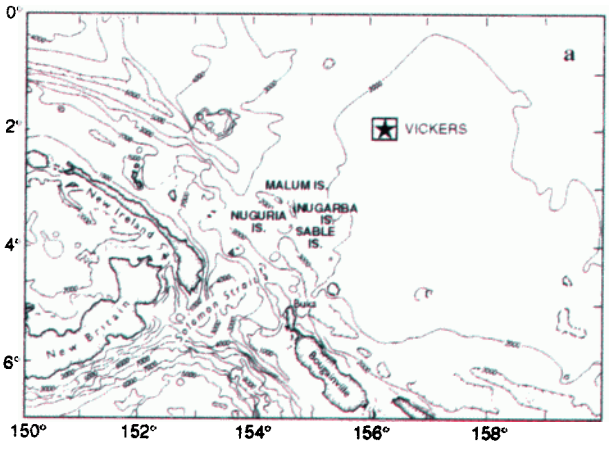

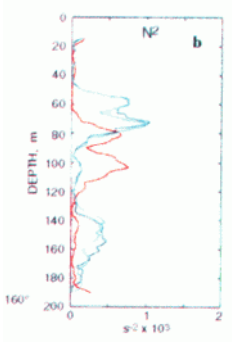

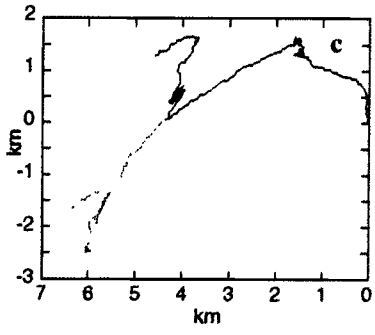

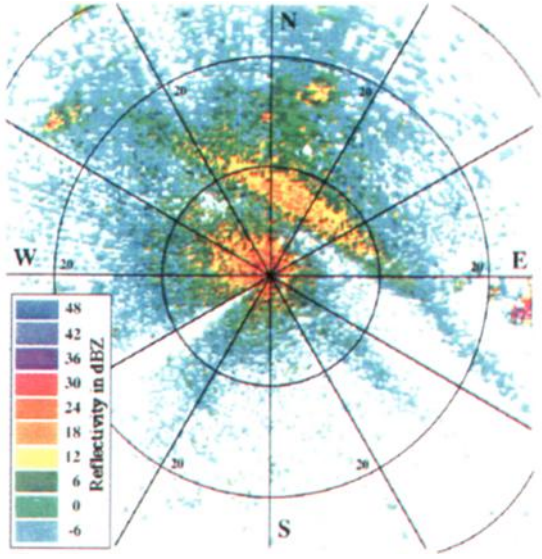

Figure 1a) The TOGA COARE domain. The suspected generating site for the upper ocean baroclinic tide and associated non-linear waves is to the southwest. The R/V Vickers maintained station at 2°S, 156° 15' E, relocating every time she drifted more than 15 km.

b) Representative profiles of squared Vaisala frequencies $N^2 = g/\rho\,(\partial\rho/\partial z)$ for the COARE site. Here, g is the acceleration of gravity and ρ is the potential density. Regions of high stability are found at 60-80 and 140-180 m (blue lines). The entire density field is displaced vertically (red line) during soliton passage, with relatively little distortion.

c) The Vickers' drift track during the passage of the January 11 event was initially toward the southwest. With the passage of the three solitary wave crests this drift was substantially arrested. If the displacements specifically associated with the three crests are removed (light line), the ship would have traveled an additional 3 km to the southwest.

d) A sea clutter image for 7 February, 1993, obtained from the MIT Doppler radar on the Vickers. Range rings are at 10 kilometer intervals. Two wave crests are seen, propagating toward the NE. Radar returns are enhanced in zones of increased ocean wave energy at .025 m wavelength or increased wave breaking. Straining of the sea-surface by solitary waves can cause both phenomena. Signatures are not seen during periods of calm, in the absence of a pre-existing surface wavefield.

February, the pattern was nearly identical, with 2,2,2,3,3, and 2 crests arriving. Often, the trailing crest was quite small.

We focus on the packet of 11 January 10:00 - 13:00 UTC, as representative of the COARE solitons. The component of ocean velocity in the direction of soliton travel is presented in Fig. 2a. The velocity is given relative to the earth, but in the advected reference frame of the ship, as displaced by the passing waves. The distortion resulting from this advection is of order u/c, which is usually much smaller than its maximum value, ~.3.

The three wave crests appear ordered in amplitude. The largest has a horizontal velocity which exceeds 0.8 m s^{-1} relative to the earth and 1.0 m s^{-1} relative to the background mixed layer. The crests are spaced by ~50 min. However, the ship was apparently displaced by ~3 km relative to a mixed layer (Fig. 1c) with the velocity pulses "removed". At a fixed position, the interval between crests would be reduced by approximately 10 min.

The packet passage occurs against a background internal tide which crests around 08:00 UTC, as evidenced by the vertical displacement of the horizontal velocity field. Surface layer (0-80 m) currents continue toward the S.W. for several hours following the first crest, transitioning to a N.E. flow only after passage of the third soliton. This bore-like behavior is reminiscent of observations of Osborne and Burch, 1980. In COARE, the asymmetry of the tide was most pronounced in the surface layer, less so at depth.

The two dimensional nature of solitary waves $(u = u(z,\phi), \text{where} \phi = x - ct)$ (Benjamin, 1966), when coupled with the ability to measure absolute velocity, present a unique opportunity. The stream function, ψ, of the flow, where $\partial\psi/\partial z = c - u$, $\partial\psi/\partial x = w$, can be inferred directly from the observations. The calculation is facilitated by the assumption that $\partial/\partial x = c^{-1}\,\partial/\partial t$. The phase speed, c, is a free parameter which is set from the observations. For $c >> u$, the results are not sensitive to its assumed value.

Inferred streamlines, contours of constant ψ, are given in Fig. 2b. Jitter in the vertical displacement of the deep streamlines results from GPS error. The streamlines are plotted against a background of acoustic scattering intensity which has been corrected for inverse square spreading and attenuation. Intensities

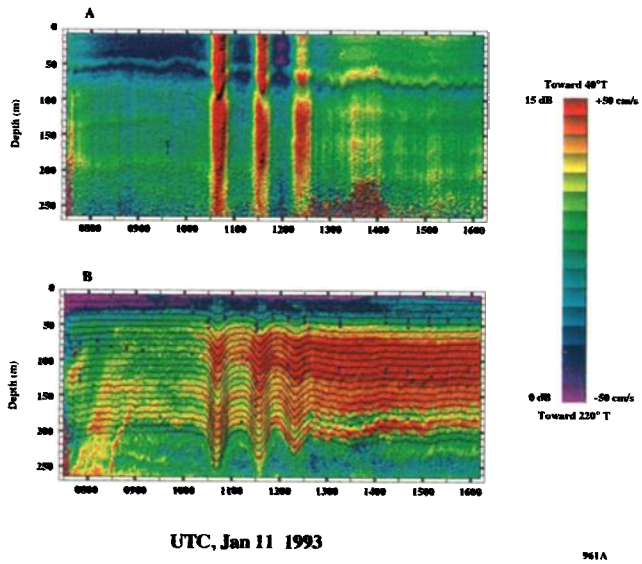

Figure 2 a) The along-path (NE-SW) component of absolute ocean velocity for the 11 January event. Color indicates current speed. The grayscale shading is proportional to current shear. Sonar precision decreases below 200 m, a consequence of low signal level at great range. The fine vertical stripes are the signature of GPS error.

b) The acoustic scattering strength field at 161 kHz. Calculated flow streamlines are superscribed in black. Regions of the water column with unstable density gradient are indicated by the purple rectangles.

are presented on a logarithmic scale relative to an arbitrary standard. The full range of the scale represents variation of a factor of 30.

The intensity record shows the arrival of the nocturnal zooplankton migration at local dusk, 08:00 UTC. From 09:00 through 10:20 the scattering field evolves but little. The solitons are seen to depress the scattering layers. Observed vertical displacements are in good agreement with the calculated streamlines. Correspondence degrades following the third crest. Apparently, the assumption of non-dispersive 2-d flow is not justified in this region.

Acoustic scattering strength increases in the core of the first soliton, decreases following its passage, and then increases with the passage of each subsequent crest. Scattering levels remain high for more than four hours following the last crest in the packet. Evidence of increased scattering is present in all soliton observations, both day and night.

We suggest that Bragg scattering from micro-scale (.46 cm) fluctuations in the sound speed field is responsible for the increase in acoustic return (Thorpe and Brubaker, 1983, Goodman, 1990, Seim and Gregg, 1995). The increased structure in the associated temperature and salinity fields is a consequence of local turbulent events which follow passage of the solitons. This interpretation is supported by the relative uniformity of scattering in the surface mixed layer. In such an isothermal, isohaline region, turbulent motion does not produce the fine-scale fluctuations required for increased Bragg scattering (Thorpe and Brubaker, 1983).

The "turbulence" fails to decay in the hours following soliton passage. We note that salinity structures at the Bragg scale can be responsible for much of the scattering increase (Seim and Gregg, 1995). A characteristic diffusive decay time for salinity structure is of order $\lambda_B^2/\upsilon_s \approx 5$ hrs, where λ_B is the Bragg length scale, and υ_s is the molecular diffusivity of salt. Long after active turbulence ceases, elevated scattering levels should persist. The salinity fine structure acts as a nearly passive tracer, providing an "acoustic dye" which marks the advective stirring following event passage.

Profiles of density, temperature and salinity have been obtained at 20 minute intervals to a depth of 180 m throughout the passage of the January solitons. The purple rectangles in Fig. 2b represent regions where unstable density gradients are encountered. The gradient is here determined as a 5 meter first difference. Persistent overturning is seen at the base of the surface layer (45-60 m), and in a layer centered at 110 m. The overturning in these layers precedes the arrival of the solitons, emphasizing the marginal dynamic stability (Miles, 1963) of the equatorial currents. The 11:30 profile coincides with the passage of the second crest. Multiple overturns are observed between 120 m and 180 m, as well as in the weakly stratified layer.

3. Event Evolution

Liu et al., 1985, demonstrated numerically that under appropriate conditions, a fairly arbitrary upper layer current jet (in a two layer fluid) would evolve into a train of deep water solitary waves. They suggested that barotropic (surface) tidal flow near the Pearl Bank produced the surface jet which was responsible for the Sulu Sea solitary waves. Observations in the Bay of Biscay prompted New and Pingree, 1990, to suggest that the solitary wave trains evolve as an instability, not on an arbitrary disturbance, but on the internal tide itself. Recent modeling studies (Gerkema and Zimmerman, 1995) explore this conjecture.

The downward cresting solitons appear at the Vickers site several hours after the observed upward crest of the semi-diurnal baroclinic tide. Is this co-occurrence coincidental, or are the two phenomena closely coupled? A long-term perspective can be obtained from moored time series data collected at 2S, 156E. The mooring, deployed as part of the Tropical Atmosphere Ocean (TAO) Array (McPhaden, 1993), was specially instrumented with a dense vertical array of temperature and salinity sensors for deep ocean validation of the TOPEX/POSEIDON satellite altimeter mission. The time series provide estimates of the volumetric variations in water masses with 5-minute temporal resolution. From these, changes in sea-surface height can be inferred to an accuracy of 1-2 cm (Picaut et al., 1995).

Fig. 3a shows a three-day estimate of this "dynamic height", relative to 1692 m, obtained in September 1992. A clear relationship between the "solitary" waves and the underlying tide is seen. During January 1993, dynamic height estimates from the TAO mooring also show the passage of non-linear waves. However, the variability from tide to tide is greater in January than in September.

When dynamic height calculations are repeated for the January 11 event using the Vickers density data, estimates of .1 m relative to 170 m depth (the maximum depth of the density profile) are obtained. However, if the observed fluid acceleration at 170 m is ascribed to a pressure gradient resulting from variable sea-surface elevation, a height estimate comparable to the TAO observations is obtained (Fig. 3b). Coupled with the 1 km approximate horizontal length scale of the crests, sea-surface slopes of 5×10^{-4} are implied. Isopycnal slopes of 5×10^{-2} are seen in the thermocline.

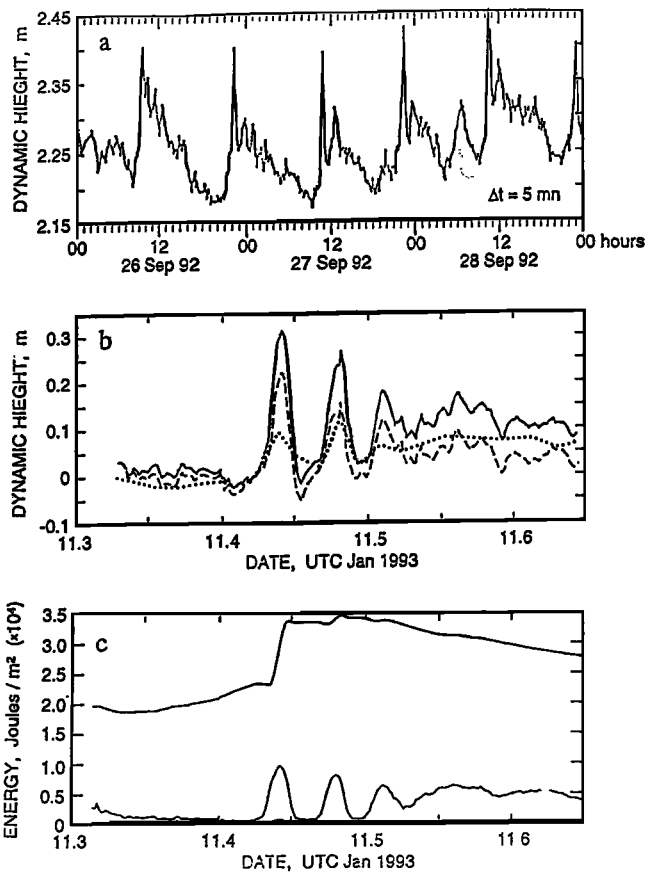

Figure 3 a) The dynamic height of the sea-surface relative to 1692 m, as estimated from temperature data at the TAO mooring at 2 S, 156 E. The record, from September 1992, illustrates the close link between the "solitary" waves and the underlying tide.

b) The sea-surface dynamic height relative to 170 m for the 11 January event, can be estimated from Vickers density data (dotted line). The sea-surface displacement required to produce the observed horizontal acceleration at 170 m is given by the dashed line. The actual displacement is estimated as the sum of the two effects (solid line).

c) Kinetic energy (top) per unit area and potential energy (bottom) for the 11 January event. Motion from the sea-surface to 170 m is considered. The contribution to potential energy from sea-surface displacement is given by the light line.

4. Energetics

Central to the issue of wave energetics is the definition of an appropriate unperturbed background state. For a potential energy calculation it suffices to use the calculated flow streamlines as surrogate isopycnal surfaces. In determining kinetic energy, we consider only the component of absolute water velocity in the direction of propagation, making no attempt to separate the soliton/bore motion field from the underlying tide.

Estimates of kinetic and potential energy are presented in Fig. 3c. These are based on integrations over the top 170 m, the region sampled by the CTD.

The contribution to soliton energy from depths greater than 170 m can be inferred using theoretical mode-one waveforms for vertical displacement and horizontal velocity, (Gill, 1982, eqns. 6.9.19, 6.10.2). The energy per unit area of the full-depth flow is a factor of 1.1 (kinetic) and 2.2 (potential) greater than the values given in Fig. 3c. The total energy found in the three-wave solitary group is approximately 10% of that in the underlying baroclinic tide. Solitary wave formation represents an efficient means of energy transfer from the tidal band to higher frequency motions.

5. Summary

We observe a series of extremely energetic deep-sea solitary waves propagating north-eastward through the Warm Pool of the Western Tropical Pacific. The apparent generation site is in the vicinity of the Nugarba Islands, 3° 30'S, 154° 30'E. The waves are phase locked to the underlying baroclinic tide, which itself is extremely non-sinusoidal.

The solitons appear to interact minimally with the larger scale Equatorial Current System. The Equatorial Undercurrent is simply displaced vertically by their passage. This "advective displacement" contrasts with the more common principle of "linear superposition" which is generally applicable to lower energy fluid phenomena.

The intrinsic shear and strain of the solitary wave is sufficient to trigger shear instability in the weakly stratified region 40-80 m depth. (However, observations of critical Richardson number are wide-spread, associated with the strong pre-existing shears). Distinct increases in acoustic scattering strength are observed following passage of all of the solitons, suggesting the creation of fine-scale sound-speed (salinity) fluctuations.

It is unclear whether the energy which creates this microstructure is extracted from the solitons, the underlying baroclinic tide, or the pre-existing flows. Even a modest energy loss from the solitons (10% per 100 km) is sufficient to support vertical heat fluxes of order 16 Watts/m^2 in this region of the Warm Pool during periods of spring tide. Such fluxes can introduce significant temporal and spatial inhomogeneity in the larger scale oceanography of the region.

Acknowledgments. We thank Capt. Schneible, Mr. Benson and the crew of the R.V. John Vickers for their excellent support. Eric Slater, Lloyd Green, Mike Goldin and Chris Neely designed, constructed and operated the SIO Doppler sonar. This work was supported by the TOGA Program of NSF/NOAA, as well as the NASA-ORSTOM Noumea TOPEX Poseidon Validation Project.

References

Apel, J.R., J.R. Holbrook, A.K. Liu, and J.J. Tsai, 1985, The Sulu Sea Soliton Experiment, J. Phys. Oceanogr., 15, 1625-1651.

Benjamin, T.B., 1966, Internal waves of finite amplitude and permanent form, J. Fluid. Mech., 25 II, 241-270.

Gerkema, T., and J.T.F. Zimmerman, 1995, Generation of nonlinear internal tides and solitary waves, J. Geophysical Res., 25, No 6, 1081-1094.

Gill, A.E., 1982, Atmosphere-Ocean Dynamics, Academic Press, London, equations 6.9.19, 6.10.2

Goodman, L., 1990, Acoustic Scattering from Ocean Microstructure, J. Geophys. Res., 95, 11557-11573.

Haury, L.D., M.G. Briscoe, and M.H. Orr, 1979, Tidally generated internal wave packets in Massachusetts Bay, Nature, 278, 312-317.

Holloway, P.E., 1987, Internal Hydraulic Jumps and Solitons at the Shelf Break region on the Australian North West Shelf, J. Geophys. Res., 92, 5405-5416.

Liu, A.K., J.R. Hollbrook, and J.R. Apel, 1985, Non-linear internal wave evolution in the Sulu Sea, J, Phys. Oceanogr., 15, 1613-1624.

McPhaden, M.J., 1993, TOGA-TAO and the 1991-93 El Niño-Southern Oscillation event, Oceanography, 6, 36-44.

Miles, J., 1963, On the stability of heterogeneous shear flows, J. Fluid Mech., 16, 209-227.

New, A.L., and R.D. Pingree, 1990, Large Amplitude internal soliton packets in the central Bay of Biscay, Deep Sea Res., 37, 513-524.

Osborne, A.R., and J.L. Burch, 1980, Internal solitons in the Andaman Sea, J.L. Science, 208, 451-460.

Picaut, J., A.A. Busalacci, M.J. McPhaden, L. Gourdeau, F.I. Gonzalez and E.C. Hackert, 1995, Open Ocean validation of TOPEX/Poseidon sea level in the western equatorial Pacific, J. Geophys. Res., 100, C12, 25109-25127.

Pinkel, R., and J. Smith, 1992, Repeat sequence codes for improved performance of Doppler sodar and sonar, J. Atm. Ocean. Tech, 9, 149-163.

Sandstrom, H., and J.A. Elliot, 1984, Internal tide and solitons on the Scotian Shelf: a nutrient pump at work, J. Geophys. Res., 89, 6415-6426.

Seim, H., and M. Gregg, 1995, Acoustic backscatter from turbulent microstructure, J. Atm. Oceanic Tech., 12, 367-380.

Thorpe, S.A., and J.M. Brubaker, 1983, Observation of sound reflection by temperature microstructure, Limnol. Oceanogr., 28, 601-613.

Webster, P.J., and R. Lukas, 1992, TOGA COARE: the Coupled Ocean Atmosphere Response Experiment, Bull. Amer. Meteor. Soc., 73, 1377-1416.

(Received: February 28, 1997; Accepted: May 1997.)